

The Processing of Kinetic Contours in the Brain

S. Zeki, R.J. Perry and A. Bartels

Wellcome Department of Imaging Neuroscience, University College London, London WC1E 6BT, UK

This work investigates whether the brain assigns special cortical areas for the processing of kinetic contours. In human imaging experiments, we compared the brain activity produced in the so-called 'kinetic occipital' area ('KO') when humans perceive shapes generated from kinetic boundaries or from equiluminant colors. 'KO' was activated whenever subjects perceived shapes, no matter how they were derived; it is therefore not specialized for the processing of kinetic contours. The application of independent component analysis (ICA) to imaging data obtained when subjects viewed 22 min of an action movie showed that the time course of activity in 'KO' correlates better with activity in area V3 than with activity in two adjacent areas, V5 and LO. We thus consider 'KO' to be part of the V3 family of areas, and use the terminology of Smith *et al.* (J Neurosci 18:3816–3830, 1998), to refer to it as area V3B. Recordings from orientation-selective cells in the macaque V3 complex show that the great majority have the same orientational specificity when tested with oriented lines generated from kinetic stimuli or from luminance differences. We conclude that there is no present evidence for a visual area specialized for the processing of kinetic contours in the primate visual brain.

Introduction

The brain can easily perceive forms in motion and construct forms from motion, but how it does so is not clear. One suggestion is that areas of the V3 complex are heavily involved in the recognition of dynamic forms, i.e. forms in motion or derived from motion (Zeki, 1991), which is not to say that they alone are engaged in executing this difficult task. The cells of the two constituents of the V3 complex in the macaque, areas V3 and V3A, are overwhelmingly orientation selective, indifferent to the color of the stimulus and optimally responsive when the oriented line moves orthogonally to the preferred axis of orientation (Zeki, 1978; Burkhalter and Van Essen, 1986). This, together with evidence derived from other systems and reviewed below, has led to the more general formulation that an area of the visual brain is capable of drawing on signals from any source to execute its specialized function (Zeki and Shipp, 1988). If this formulation is correct, one would suppose that the cells of the V3 complex are capable of responding to lines of specific orientation, no matter how these are generated. They should therefore have the capacity to draw on the form and the motion systems, and retain their specificity whether the lines they respond to are generated from luminance differences, kinetic contours or equiluminant color boundaries. Anatomical evidence shows that the cells of V3 can indeed draw upon signals from the M or the P systems (Casagrande and Kaas, 1994; Callaway, 1998), thus endowing them with the potential of responding to inputs from a variety of sources. This strategy of tapping information from any source to construct a visual attribute seems to be a general one used by the visual brain. It is well demonstrated by several studies in different visual areas which, collectively, give credibility to the general principle of 'cue invariance' in cortical

processing, by which is meant the ability of cells in an area to respond to their preferred stimulus, however it is derived (Albright, 1992; Orban *et al.*, 1993; Sary *et al.*, 1993; Geesaman and Andersen, 1996; Grill-Spector *et al.*, 1998; Okusa *et al.*, 2000). There is, however, an alternative view that merits consideration. This supposes that the brain treats kinetic boundaries as an entirely separate visual attribute, distinct from both motion and form, and therefore devotes a specialized system, including a specialized cortical area, to it. This view was first proposed by Gulyas *et al.*, who believed that they had identified areas that show differential involvement to contours defined by motion as compared to contours from color (Gulyas *et al.*, 1994). However, the methodology they used to analyze their imaging results has been criticized, compromising their conclusions (Frackowiak *et al.* 1996; Roland and Gulyas, 1996). More recently, Van Oostende *et al.* expressed this view more emphatically, and described an area that they consider to be 'specialized in the processing of kinetic contours' which they have named 'KO' (kinetic occipital), thereby reflecting their belief in its specialization (Van Oostende *et al.*, 1997).

Such a putative specialization opens up a host of interesting questions regarding the construction of forms by the brain, which we wanted to explore. But we wanted, first, to be certain of the specialization of 'KO' and thus ascertain that the brain does indeed use a specialized cortical area to construct forms from kinetic contours. 'KO' has not been studied for its involvement in the generation of forms and shapes from attributes other than luminance and kinetic contours, e.g. color. One aim of our imaging experiments was therefore to compare the responses of 'KO' to simple shapes generated from kinetic boundaries and from isoluminant colors because much work suggests that these two systems are the ones that are most separate from each other in terms of cortical representation, even though there are cross-connections between them (Shipp and Zeki, 1989; Zeki and Shipp, 1989; Lund *et al.*, 1994). If 'KO' is specialized for kinetic contours, one would expect it to be less reactive, or even unreactive, to contours generated from static equiluminant colors. On the other hand, if an area specialized for the construction of forms is able to draw on signals from any source to undertake its function, one would expect that shapes constructed from equiluminant colors would also activate 'KO', as indeed would shapes generated from static textures.

We also hoped to resolve another uncertainty about 'KO', namely its relationship to other visual areas in its vicinity. There is little doubt from the published evidence that 'KO' is distinct from the more anteriorly located V5, specialized for visual motion (Zeki *et al.*, 1991; Watson *et al.*, 1993; Sereno *et al.*, 1995; Tootell *et al.*, 1996). What is more problematic is its relationship to areas of the V3 complex (V3 and V3A) (Shipp *et al.*, 1995; Tootell *et al.*, 1997) and to the complex of areas that constitute LO (Malach *et al.*, 1995). The former are areas that

have been considered to constitute part of the (dynamic) form system of the visual brain (Zeki 1978, 1991). Their proximity to 'KO' naturally raises the question whether 'KO', assuming it to be an entirely separate area, could plausibly belong to the V3 family of areas, as was indeed implied by the use of the alternative name for 'KO', 'area V3B' by Smith *et al.* (Smith *et al.*, 1998). In the study of Van Oostende *et al.*, activity in 'KO' is not much different from that in V3A, except that the latter was found to be less reactive to luminance borders compared to 'KO' (Van Oostende *et al.*, 1997). In the study of Smith *et al.*, V3 and 'KO' were equally active to second-order motion stimuli, which is what led Smith *et al.* to refer to 'KO' as V3B (Smith *et al.*, 1998). The relationship of 'KO' to the LO complex, an area that is critical for visual object recognition (Malach *et al.*, 1995), is also uncertain. If 'KO' is indeed distinct from LO, then a compelling case for it has not been made by the published maps, which show a substantial and sometimes total overlap between the two (Van Oostende *et al.*, 1997). Hence, another possibility is that 'KO' belongs to the LO family of areas.

To address this issue, we applied the independent component analysis (ICA) method of Bell and Sejnowski (Bell and Sejnowski, 1995) to functional imaging data acquired when humans viewed dynamic complex visual scenes (Bartels and Zeki, 2001, 2003). This method isolates cortical areas with respect to their activity time course (ATC), placing areas that have different ATCs in separate independent components (ICs). This time-based parcellation of the cortex is done without *a priori* hypotheses (McKeown *et al.*, 1998) and has the advantage of showing which areas have ATCs that correlate. Any evidence that the ATC of 'KO' is distinct from those in LO, the V3 complex and the V5 complex would be a strong hint that 'KO' operates independently from other areas and thus deserves a separate status, regardless of whether it is specialized for processing kinetic contours or not. On the other hand, there was always the possibility that the ATC of 'KO' might correlate better with one of the other areas, such as V5 or V3 or LO, thus betraying its status as belonging to one family of areas or another.

Results obtained from these imaging experiments encouraged us to examine the responses of orientation-selective cells in the areas of the V3 complex (V3 and V3A) of the macaque to kinetic and luminance boundaries. The presence in the V3 complex of cells that are only selective for oriented lines when generated from kinetic contours would be strong suggestive evidence that a separate system, embedded within the V3 complex, processes oriented lines so generated. The choice of the V3 complex was not arbitrary. Apart from the functions imputed to it and alluded to above, the results of our imaging studies emphasized the need for a study of selectivities within the V3 complex.

Our overall conclusion from all these results is that 'KO' (V3B) is not specialized for the processing of kinetic contours and that it belongs more properly to the V3 family of areas. We conclude that the brain does not devote a cortical area specifically to the processing of kinetic boundaries.

Materials and Methods

For both imaging studies informed consent was obtained from all subjects in accordance with the Declaration of Helsinki, and ethical approval was granted by the Ethics Committee of the National Hospital for Neurology and Neurosurgery, London, UK.

Stimuli and Task for Functional Magnetic Resonance Imaging (fMRI) Experiment 1

Experiment 1 used eight normal subjects (six male, seven right-handed) to compare the patterns of activity in the brain when subjects viewed shapes derived either from color or from motion cues. The four types of

stimulus, and the design of the experiment, are illustrated in Figure 1. 'Color shapes' (CS), such as the keyhole in the center of Figure 1A, were constituted from static isoluminant red and green oriented bars, by arranging the orientation of the bars inside the shape to be orthogonal to those outside. Color shapes could only be extracted by a visual subsystem that discriminates between isoluminant red and green. An equal number of 'color no-shapes' (CN) were shown, in which the background alone was present, as in Figure 1B. In both cases the orientation of the background bars was randomized between the two diagonals (tilting right or left) from trial to trial. Thus the critical difference between the two is the appearance of a simple recognizable shape in one (A) and its absence in the other (B).

The red and green bars were made isoluminant to the gray level psychophysically, using the method of heterochromatic flicker photometry (Kaiser, 1991), as follows. In the scanner, just prior to each scanning session, subjects viewed a $5.5^\circ \times 5.5^\circ$ square which, like the stimuli, was centrally presented, and alternated between gray [equal RGB values, corresponding to CIE (CIE, 1931) coordinates (x, y, z) of 0.96, 1.14, 1.26] and red (i.e. variable 'red' RGB channel, with other two channels set to zero). This square was presented on a black background. The luminance of the red was adjusted manually by the experimenter in the MRI control room, under the verbal instructions of the subject within the scanner, until the subject's perception of flicker between the red and the gray was minimized. Across subjects, the mean CIE coordinates (with the standard error of the mean, SEM) for this point were 2.21, 1.07, 0.06 (SEM 0.15, 0.08, 0.00). A similar method was then used to find an isoluminant green color (adjusting the 'green' RGB channel, with red and blue channels set to zero), which gave a green of mean CIE coordinates 0.48, 1.19, 0.04 (SEM 0.05, 0.13, 0.00). The CIE coordinates were obtained by calibrating the projector using a Spectra-Colorimeter Model PR650 (Photo Research, Chatsworth, CA). This experiment addressed the general issue of whether V3B ('KO') responds more specifically to kinetic contours than to static contours. Even though we took great care to generate the static contours from isoluminant colours, we could equally well have used contours generated from luminance instead, as did Van Oostende *et al.* (Van Oostende *et al.*, 1997).

An example of a 'motion shape' (MS) is shown in Figure 1C. Here the stationary shape is defined by kinetic contours, through the direction of motion of a field of dots, illustrated by smeared dots in this figure. Dots inside the 'shape' moved in one of the four diagonal directions, determined at random, while those outside moved in an orthogonal direction. The parameters of the dots are shown in the legend to Figure 1. The shape derived from kinetic contours was much more clearly visible in the moving display than in the stationary illustration given here, but it would be entirely invisible in any single stationary frame taken from the stimulus. As before, an equal number of 'motion no-shape' (MN) displays were shown (Fig. 1D), composed of the background alone, which in this case was simply a field of random dots all moving in the same direction (translational motion). The critical difference between the two, again, is the appearance of a recognizable shape in one (Fig. 1C) and its absence in the other (Fig. 1D). These four conditions form a 2×2 factorial design (Fig. 1), in which the two factors are shapes versus no-shapes and motion versus color.

Subjects fixated a central black cross throughout the experiment, and displays in which this cross appeared on a uniformly gray background ('gray' stimuli) were included as a baseline condition. Trials were grouped into 'epochs' consisting of 10 stimuli of the same configuration (e.g. color shapes). Each stimulus was presented for 500 ms, and followed by a gray screen for 1100 ms, up to the onset of the next stimulus. Before scanning, subjects were trained to recognize a 'keyhole' shape as the 'target' (Fig. 1A). During scanning, the subject's task was to press a button with their right index finger whenever they saw this target shape, but not to press to other 'distractor' shapes. The target object was randomized with eight distractor shapes, giving a mean target frequency of 11% (1/9). Subjects were told beforehand that there would be periods during which no shapes would be present on the screen (i.e. during no-shape and gray epochs), and that no response was required during these periods.

All of the statistics in the present study are based on these four types of epoch: CS, CN, MS and MN. Four types of epochs with other stimulus configurations were also included as part of a separate study (Perry and Zeki, 2000). Epochs were pseudo-randomized with the constraint that,

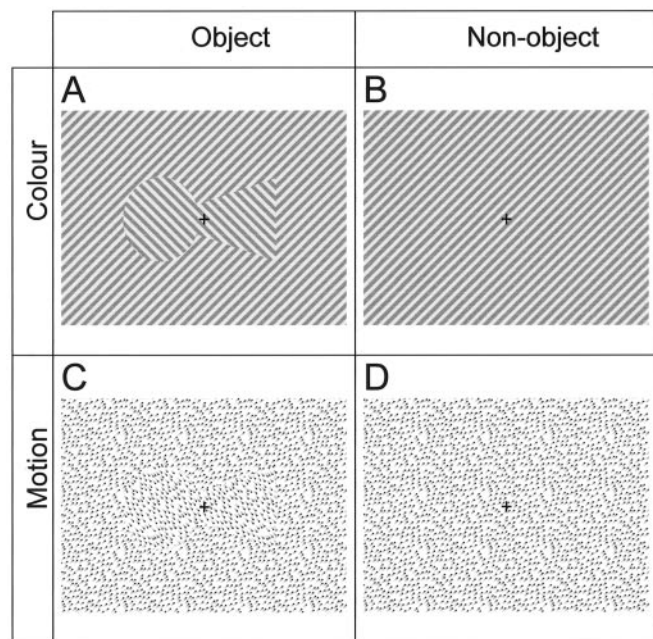


Figure 1. Illustration of stimuli and 2×2 factorial design. The shape shown in the left column is the 'target' shape (a keyhole). (A) Color shape (CS). The screen was composed of alternating bars of isoluminant red and green, the orientation of the lines inside the shape lying orthogonally to those outside. (B) Color no-shape (CN). The same background as CS, but without the central shape. (C) Motion shape (MS). The screen was composed of a random field of moving dots, which are represented here by smeared dots. Dots inside the object moved in a direction orthogonal to those outside. The dots had the following properties: dot size 0.05° ($= 1$ pixel), density 20%, speed $0.5^\circ/s$ (11 pixels/s), dot lifespan ∞ , motion coherence 100%. (D) Motion no-shape (MN). The same background as MS, but without the central shape.

during the whole experiment, subjects saw nine epochs of each type, and 18 'gray' epochs. These 90 epochs were shown in two equal blocks, with a short rest between. Subjects were familiarized with the target shape, trained on the task, and given 10–15 min of practice outside the scanner until they were confident. During scanning most of the target shapes were correctly identified (Table 1). The subjects appeared to find extracting objects from motion more difficult. If anything, this would tend to enhance the response to motion objects relative to color objects, which was not observed in our data.

Stimuli and Task for fMRI Experiment 2

The aim here was to learn the degree to which the ATC of V3B ('KO') correlates with that of other areas and, if so, which ones. This is best achieved by studying the activity in V3B in complex free-viewing conditions, over a relatively prolonged period of time. Exposure to a complex stimulus has the advantage that many areas will be differentially active in time over the viewing period (Bartels and Zeki, 2001, 2003). For this second study we therefore asked eight normal subjects (three male, all right-handed) to view the first 22 min 25 s of the James Bond movie *Tomorrow Never Dies*, including its sound track. The movie was interrupted eight times (i.e. every 2.5 or 3 min) with a blank period (black screen, no sound) lasting 30 s as a baseline condition. As part of a separate study, the movie changed from colour to black and white every 30 s.

Image Acquisition and Pre-processing (Experiments 1 and 2)

Subjects were scanned in a 2 T Magnetom Vision fMRI scanner with a head-volume coil (Siemens, Erlangen, Germany), while viewing the $26^\circ \times 19^\circ$ visual display via an angled mirror. A gradient echo-planar imaging (EPI) sequence, with an echo time (T_E) of 40 ms and a repeat time (T_R) of 4.1 s was selected to maximize blood oxygen level dependent (BOLD) contrast. Each brain image was acquired in 48 slices, approximately 2 mm thick with 1 mm gaps in between, and each comprising 64×64

Table 1

Means and sample SDs (between-subjects) of percentage scores across all eight subjects while they were being scanned during experiment 1

	Targets (40 per subject)		Non-targets (320 per subject)	
	Hits (%)	SD (%)	Correct rejections (%)	SD (%)
Color objects	92.5	10.4	99.7	0.6
Motion objects	67.5	21.9	96.6	6.2

For subject 3 the file containing scores from session 2 was corrupted, so scores for this subject are based on session 1 only.

pixels. The number of EPI scans per subject was as follows: experiment 1, 180 scans; experiment 2, 324 scans (subjects 1–4) or 368 scans (subjects 5–8). The data were pre-processed using the SPM99 software (Wellcome Department of Imaging Neuroscience, London). In experiment 2, the data were realigned in time using sinc interpolation (Schanze, 1995). In both experiments the EPI images were spatially realigned and normalized to the Montreal Neurological Institute template provided in SPM99 [which approximates to the Talairach–Tournoux atlas (Talairach and Tournoux, 1988)] and spatially smoothed with an isotropic Gaussian kernel of 10 mm (experiment 1) or 6 mm (experiment 2). After spatial pre-processing, non-physiological high-frequency noise was filtered out with a low-pass filter shaped to the spectral characteristics of the canonical hemodynamic response function (HRF) within SPM99. In experiment 1, an additional high-pass filter with a period of 512 s was used to remove low-frequency noise. The signal in every voxel was divided by the mean signal intensity of each whole image (global normalization), to compensate for fluctuations of the global signal.

Epoch-based Statistical Analysis (Experiment 1)

Each epoch type was modeled with a separate box-car function (convolved with SPM99's canonical HRF) in a multiple regression analysis (Friston *et al.*, 1995). In addition, subjects' responses during scanning were recorded, classified as hits or false positives, and modeled in the design matrix as events of no interest [using the HRF and its first temporal derivative (Josephs *et al.*, 1997)]. Misses were modeled in the same way, but correct rejections were not modeled explicitly, to avoid over-specifying the model. Group results are based on a fixed-effects analysis, in which the reliability of the observations is assessed relative to within-subject variance, as is appropriate for establishing 'typical' features of the human brain (Friston *et al.*, 1999). The figures have been thresholded at $P < 0.001$ uncorrected to show the spatial extent of the clusters.

ICA Analysis (Experiment 2)

ICA analysis (Bell and Sejnowski, 1995) was done on each subject separately, to obtain spatially independent components (McKeown *et al.*, 1998). Based on information theory, ICA is capable of unmixing or decomposing any linear mixture of independent sources, which need not be known *a priori*. In the case of fMRI, we assume that all voxels belonging to one functionally specialized area or to a network of highly correlated areas form such an 'independent' source, several of which are spatially 'mixed' in the fMRI whole-brain images. During complex tasks, many different, and maybe temporally or spatially overlapping, sets of areas will be active, each with its own characteristic ATC (Bartels and Zeki, 2001, 2003). ICA identifies such sets by separating voxels that share similar ATCs from other voxels and saves them in a separate independent component (IC – a whole-brain image). The total number of ICs is equal to the number of input-images, in our case 324 (for subjects 1–4) or 368 (for the subjects 5–8). Each IC has an associated time-course, which corresponds closely to the BOLD signal of the most significant voxels in that IC.

The methodology we used for the ICA analysis in this and in our earlier studies (Bartels and Zeki 2000) was similar to the one of McKeown *et al.* (McKeown *et al.*, 1998), who first applied ICA to fMRI data. After pre-processing, voxels lying outside the brain were removed by manual thresholding, done for each subject individually, in order to reduce the total data to be processed. Data were then converted into a large matrix with the number of rows corresponding to the number of scans (324 for

Table 2

Talairach coordinates (Talairach and Tournoux, 1988) of the areas used in the ICA analysis of the free viewing experiment

Study	Area	x	y	z	n
This study	V3v left	-22 (-28, -19)	-90 (-94, -84)	-19 (-20, -18)	8
This study	V3v right	27 (27, 33)	-87 (-93, -81)	-18 (-19, -16)	7
This study	KO left	-30 (-31, -27)	-95 (-96, -93)	1 (-1, 2)	7
This study	KO right	32 (28, 36)	-91 (-95, -88)	3 (-0, 5)	8
This study	V5 left	-49 (-51, -48)	-75 (-78, -73)	3 (-2, 6)	8
This study	V5 right	52 (51, 54)	-69 (-71, -66)	0 (-4, 5)	8
DeYoe <i>et al.</i> (1996)	V3v	±25	-85	-15	4
Van Oostende <i>et al.</i> (1997)	KO left	-32 (-26, -36)	-92 (-88, -96)	0 (-4, 4)	17
Van Oostende <i>et al.</i> (1997)	KO right	31 (28, 34)	-92 (-86, -93)	0 (-1, 4)	20
Van Oostende <i>et al.</i> (1997)	V5 left	-42 (-40, -48)	-78 (-74, -79)	4 (-1, 4)	20
Van Oostende <i>et al.</i> (1997)	V5 right	41 (40, 44)	-70 (-67, -73)	2 (-1, 4)	20

Coordinates of areas identified in this and in previous studies (median and quartiles).

subjects 1–4; 368 for subjects 5–8), and the number of columns corresponding to the number of voxels (between 60 000 and 70 000, depending on the subject). This matrix was submitted to the ‘runica’ procedure supplied in the EEG package by Makeig (<http://www.cnl.salk.edu/~scott/ica-download-form.html>) (Makeig *et al.*, 1997), which applied ICA incorporating the natural gradient feature of Amari (Amari, 1998), using the default parameters. In each subject, we identified those ICs that contained their most significant voxels within the visual cortex, based on their anatomical position. Among those, we selected areas whose most significant voxel came closest to the Talairach coordinates described for ‘KO’ and V5 by Van Oostende *et al.* (Van Oostende *et al.*, 1997) and for V3v by DeYoe *et al.* (DeYoe *et al.*, 1996) (see Table 2). In all subjects, areas V5 and V3v were more clearly separated by ICA and therefore easier to identify than area ‘KO’. The medians and the quartiles of the coordinates of the areas identified are given in Table 2; they fall within a few millimeters of those reported in previous publications (see above). We isolated the BOLD signal time-courses from the most significant voxels in each area and calculated the correlation coefficients between them. In order to obtain ATCs related only to free viewing of the movie, those parts of the BOLD signal time-course that corresponded to the blank periods and the 30 s window following them were excluded.

Experiment 3 (Physiological Recordings)

We recorded from 100 cells in 12 cynomolgus monkeys, using standard procedures (Zeki, 1978). All cells were histologically verified to have been located within the V3 complex (V3 or V3A) (see Fig. 2). Monkeys were first given 25 mg/kg of ketamine hydrochloride and then anesthetized with pentobarbitone sodium and, after surgery, paralyzed with 0.4 mg/kg of pancuronium bromide, supplemented at the rate of 0.5 ml/h throughout the experiment. The electrocardiogram, rectal temperature and exhaled CO₂ were monitored continuously and maintained at physiological levels, and additional doses of anesthetic were administered to maintain adequate levels of anesthesia. Retinoscopy and other procedures were as described before (Zeki, 1978).

Once a cell’s preferred orientation was determined with computer-generated orientated lines, its receptive field was plotted on a monitor screen at a distance of 114 cm from the eye. More quantitative computer-controlled tests were generated using a Commodore Amiga computer and presented on a 20-in. Grundig monitor. The display resolution was 320 pixels wide by 240 pixels high, presented at distances varying from 100 to 114 cm from the subject. Refresh rate was 50 Hz; a new display frame was generated each 20 ms. A Neurolog spike trigger unit (Digitimer, Welwyn Garden City, UK) measured the firing rate of the cell and the number of spikes occurring in each 20 ms display frame period was recorded as the cell’s response. During stimulus presentation, a rectangular stimulus bar moved through the centre of the receptive field in different directions but at similar speeds. Stimulus bar dimensions ranged from 30° to 10° and speed of movement from 1° to 5°/s. Once a cell’s optimal responses were determined from luminance contours, it was stimulated with a line of its preferred orientation, width and length generated from kinetic contours and moving in two directions orthogonal to its long axis.

For the orientation-selective cells studied here (the great majority), the bar was moved across the receptive field of the cell in eight directions and responses plotted at 45° intervals, although tests were also carried out at 15°, 30°, 60° and 90° intervals. At least two such direction tests were performed on each cell. In the first, the stimulus bar was solid white on a black background (contrast > 90%); in the second, the stimulus bar contained a texture matrix and the background a second one. The textures (Fig. 3) were composed of 50% black and 50% white randomly arranged squares so that there was no overall luminance contrast. The grain of the texture was one pixel, subtending ~3’ of arc at the eye. The number of times that the line moved through the receptive field varied, depending upon the background discharge rate of the cell; it was rarely less than twice, and commonly three times or more.

Two types of moving texture (kinetic contour) stimuli were used (Fig. 3). In ‘frame’ stimuli, the textured contents of the stimulus bar moved with the bar. In ‘slot’ stimuli (which can be thought of as looking at a background texture through a moving slot in the foreground texture), the contents of the bar were either static or moved independently of the motion of the bar. In each case, the pixels changed dynamically as the edge moved across the screen. Thus some pixels changed from black to white or vice versa while some stayed the same on consecutive frames. The tests had parameters in the following ranges: minimum bar width, 6 arcminutes; maximum bar width, 6.5°; minimum bar length, 3°; maximum bar length, 11.00°; minimum bar speed, 1.20°/s; maximum bar speed, 8.57°/s. The minimum texture grain was one pixel, the maximum two pixels. In addition, we used some tests in which the motion of the pixels inside the bar was either parallel to that outside, though in the opposite direction, or orthogonal to it, the oriented bar itself remaining stationary. In all cases, the movement of the bar was salient and very easily perceived by the experimenter.

Our aim in these recordings was limited (i) to determining whether the cells responded as specifically to the above kinetic stimuli as they had to luminance ones; this could be done by determining the tuning curve widths of the cells in both conditions. (ii) To learning whether the cells respond as well, in quantitative terms, to the two stimuli; we determined this by obtaining quantitative data about optimal discharge rates, in terms of spikes per second, while the stimuli traversed the receptive field, for both types of stimuli. For each cell, we presented a luminance bar and a kinetic contour bar at a variety of orientations, and measured the cell’s responses. Two or three repetitions were done for each orientation in a randomized block sequence. The pairs of tests were examined in detail and, for each test, a cell response profile was drawn, using a spline interpolation between the measured orientations. The profile was used to obtain the preferred orientation, cell firing rate to that orientation and the tuning width of the preferred orientation. For the tuning width, the half width at half height of the peak response was taken. We made two statistical checks on a cell’s response to the oriented bars: (i) the cell response to each oriented bar was compared to the background firing rate of the cell using a *t*-test; and (ii) the cell’s responses to the different orientations were compared using ANOVA. In our comparison of single cells’ responses to luminance and kinetic contour stimuli (Figs 8–10),

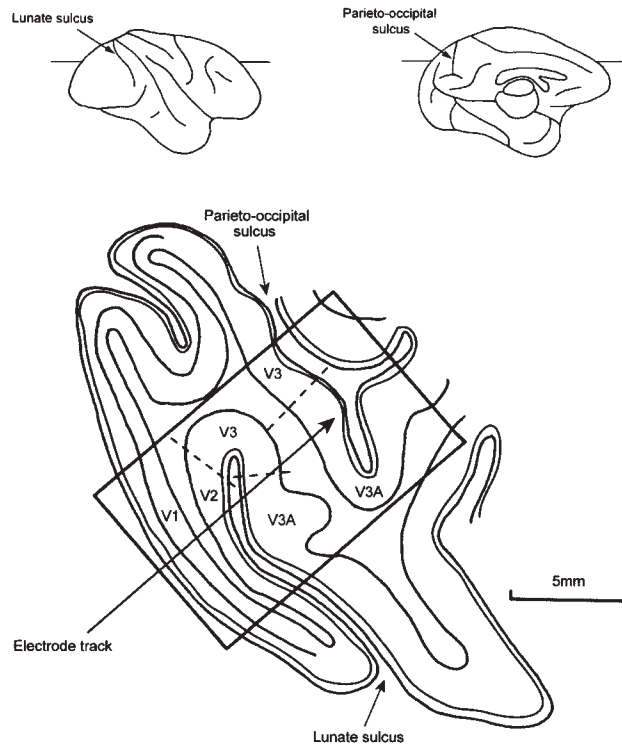


Figure 2. Diagrammatic reconstruction of a horizontal section taken through the brain of the macaque monkey, at the level indicated on the surface drawings, to show the electrode trajectories used in this study. Only the posterior part of the section is shown. For further details, see text.

only cells that showed significance at the 1% level for either kind of stimulus were included.

One or more micro-lesions were made at the site of interesting cells, by passing a 5–10 μ A DC current through the electrode for 5–10 s. At the termination of the experiment, the animals were killed by a lethal injection of anesthetic, and perfused in the standard way (Zeki, 1978). The brains were subsequently sectioned at 30 μ m and stained for Nissl substance with cresyl violet which showed the electrode tracks and the micro-lesions to advantage.

Results

Epoch-based fMRI Experiments

An area that gives its greatest response to kinetic boundaries could be doing so for one of two reasons: (i) it may be specialized for kinetic contours and thus give a response that is specific to them (Dupont *et al.*, 1997; Van Oostende *et al.*, 1997); or (ii) it may give independent responses to contours, however derived, and to motion. If (ii) is true, then there would be no specificity for kinetic contours. The simplest way to distinguish between these two alternatives is to use a factorial design, in which responses to motion and to contours (the main effects) can be dissociated from the specific response to kinetic contours (the interaction). We designed experiments based on such a 2×2 factorial design (Fig. 1). We were particularly interested in the extraction of contours in the context of shape recognition, so in our study the contours go to make up recognizable shapes.

We thought that area 'KO' should be easily identifiable, since we expected it to be active when contours must be extracted to recognize shapes (even if this were only true for motion shapes). Figure 4a shows the contrast of all shapes (which included contours to be extracted) with no-shapes (in which no contours

had to be extracted) in the group data, superimposed onto a horizontal section through the standard 'template' brain, at the level of Talairach coordinate $z = +2$. In the left prestriate cluster there is a sub-peak, at $[-32, -92, 2]$ (indicated by an arrow), which coincides almost exactly with the median coordinates of area 'KO' $[-32, -92, 0]$ (Van Oostende *et al.*, 1997). The corresponding peak in the right hemisphere (indicated by the other arrow) lies in a slightly more lateral position, at $[40, -88, 2]$ [cf. $[31, -92, 0]$ in Van Oostende *et al.* (1997)] but the same cluster extends as far medially as $[34, -92, 0]$, and is therefore also likely to be area 'KO'.

In Figure 4a.ii, the 'KO' cluster appears to be confluent with the cluster for area V5, which lies just anterior to 'KO'. Some of this confluence can probably be explained by the fact that both 'KO' and V5 will have coordinates that vary a little from subject to subject, smearing the clusters in the group data. In individual subjects, however, the 'KO' and V5 clusters tend to be distinct. Figure 4a.iii shows the same contrast for an individual subject. In this case we found that there is a clear distinction between 'KO' (at $[30, -94, 2]$, indicated by arrow) and area V5 (within which the most significant voxel in this slice is at $[-50, -68, 2]$). The peak for right 'KO' in this subject is in a slightly higher slice (at $[38, -90, 6]$), whereas the peak for V5 is in a slightly lower slice ($[48, -68, -8]$). In conclusion, we were confident that, in our contrast of shapes versus no-shapes, we could identify the area that Van Oostende *et al.* designate 'KO' (Van Oostende *et al.*, 1997), in both hemispheres.

The main purpose of the experiment, however, was to determine if there are any areas specifically involved in extracting kinetic contours. Such areas should appear in the contrast of motion shapes versus motion no-shapes (Fig. 4b.I), but not in the contrast of color shapes versus color no-shapes (Fig. 4b.II). However, they appear in both contrasts. As the direct comparison between these two contrasts shows (Fig. 4b.III), there are no areas specifically involved in extracting kinetic contours in this region of prestriate cortex, nor could we demonstrate such areas anywhere else in the brain. 'KO' does not, therefore, appear to have a specificity for kinetic contours.

This point is emphasized by examining the responses of 'KO' to the four classes of stimuli (Fig. 5). The top row of this figure shows that KO tends to give a larger response to 'motion' stimuli (MS and MN) than to 'color stimuli' (CS and CN), and a larger response to shapes (including contours, MS and CS) than to no-shapes (MN and CN). However, the lower row shows that the shape-specific response is the same whether the contours of the shape are extracted from motion or from color. In any putative area with a specificity for kinetic contours, the shape-specific response in the context of motion (MS - MN) should have been much larger than the shape-specific response in the context of color (CS - CN). 'KO' does not, therefore, appear to be such an area.

Application of ICA to fMRI Data

Area 'KO' has also been called area V3B by Smith *et al.*, because their second-order motion stimuli activated areas V3 and V3B similarly (Smith *et al.*, 1998). This similarity made us wonder whether V3B is functionally more related to area V5 (motion) or area V3 (depth and contours). The ICA method segregates cortical areas according to differences in their ATCs, assigning one or more areas to a single IC if they have similar ATCs and to different ICs if they have different ones. Many areas will be simultaneously and differentially active when viewing complex visual scenes, and we hoped that V3B would be among these. The ICA method would then place it in a separate IC or together

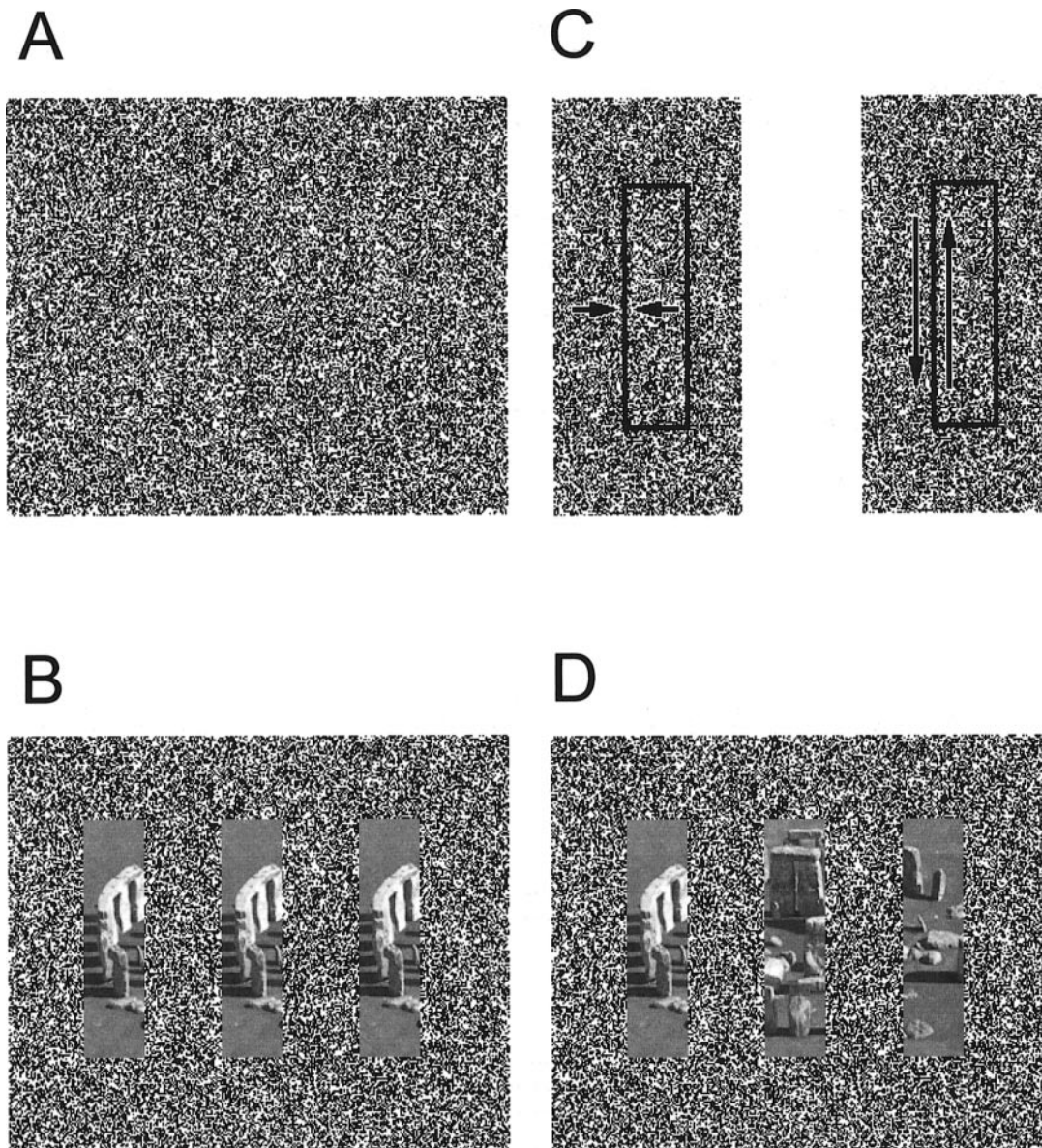
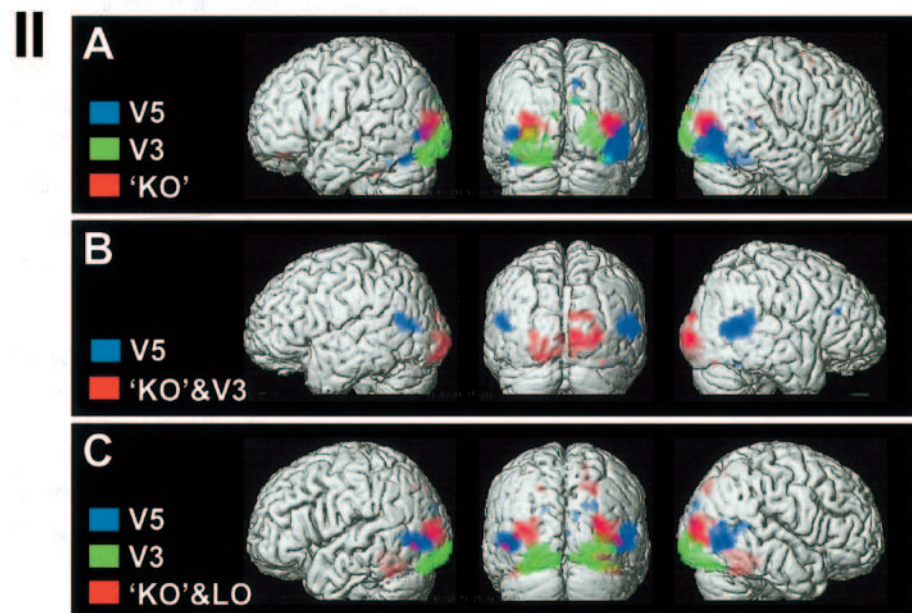
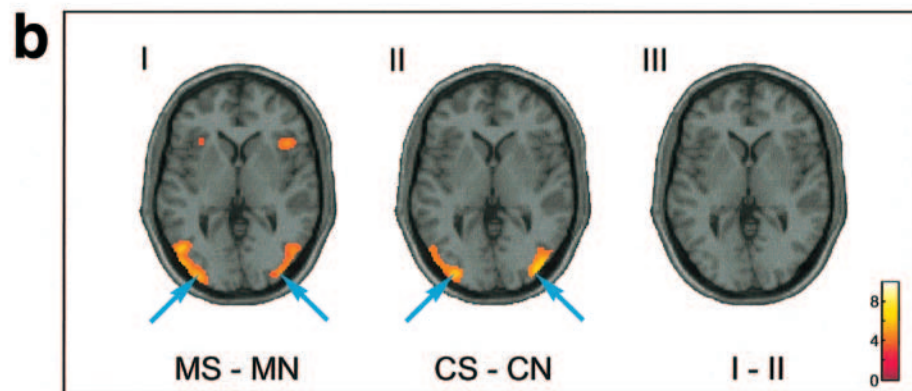
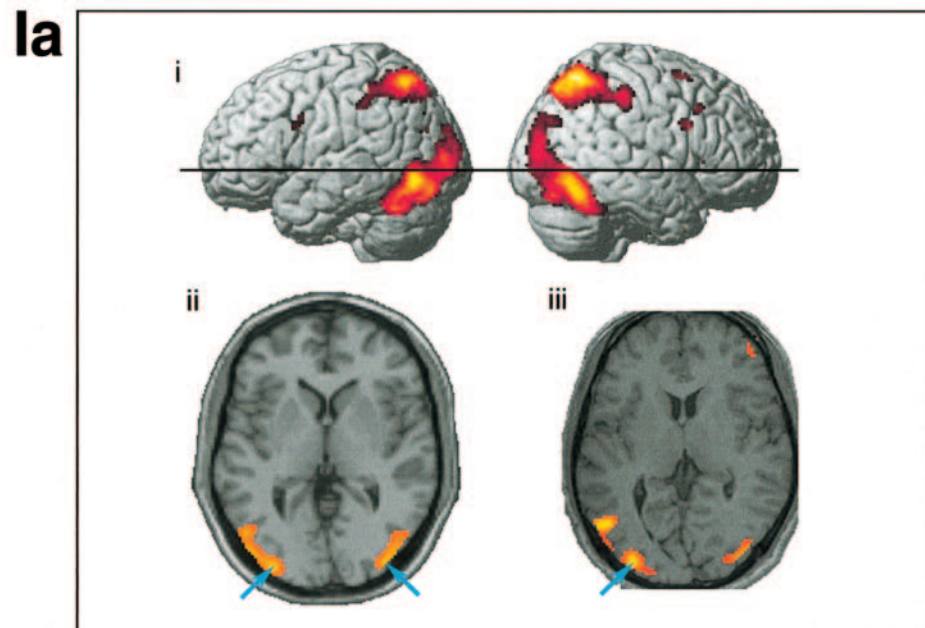


Figure 3. The kinetic contour display used to stimulate the orientation selective cells of the V3 complex in the monkey. (A) shows the grain of the texture, which consisted of a 320×240 pixel image containing a random dot matrix of 50% black and 50% white texture of grain one pixel, with each each pixel subtending 3 arcminutes at a distance of 114 cm. (B) illustrates the stimulus in 'frame mode' when the contents of the stimulus bar moved with the stimulus bar. The 'Stonehenge' image shown here and in (D) is for illustrative purposes only, and was replaced with a random texture in the actual experiment. (C) Texture motion could either be orthogonal to (left) or parallel to (right), the long edge of the stimulus bar. In some cases the textures were stationary and then the display would appear as in (A) above. (D) In 'slot mode' the contents of the stimulus bar did not move with the stimulus bar. In both the 'slot' and the 'frame' mode, the pixels at the borders changed dynamically as the stimulus bar moved, some changing from black to white or vice versa and some remaining black and some white.

Figure 4. fMRI results from the epoch study (a,b) and the ICA analysis of free viewing data (II). (Ia) Epoch study. Main effect of all shapes (color and motion) versus all non-shapes. (i) Group data rendered onto surface of standard 'template' brain supplied with SPM99. Black line shows the level of the horizontal section shown in (ii). (ii) Same data shown in a horizontal section at a level of +2 in the Talairach coordinate system with the right side of the brain shown on the right. Arrows indicate the positions of 'area KO' in each hemisphere. (iii) Same contrast shown in a single subject, superimposed onto subject's own structural scan. Arrow indicates left 'KO'. Statistical thresholds: $P < 0.05$ corrected in (i) and (ii); $P < 0.001$ uncorrected in (iii). Colors represent arbitrary scales of significance above this threshold, with lower significance shown in red, through orange, to highest levels of significance in bright yellow. (Ib) Epoch study. Modality-specific effects of shapes. (I) Contrast of motion shapes versus motion non-shapes (MS – MN). (II) Contrast of color shapes versus color non-shapes (CS – CN). (III) Direct comparison of contrast shown in (I) with contrast shown in (II) (i.e. interaction contrast [MS – MN] – [CS – CN]). Talairach coordinate $z = +2$ (as in a.ii). Arrows indicate position of area 'KO' in each hemisphere, as identified in (a.ii). Statistical threshold $P < 0.05$ corrected. The interaction contrast in (III) did not show any clusters even when the statistical threshold was dropped to $P < 0.001$ uncorrected. Scale shows relationship between color and Z-statistic. (II) ICA on free viewing data. In the free viewing experiment, ICA isolated area 'KO' either on its own, with visual area V3, or with LO, but never with V5. (A–C) show independent components of three separate subjects, which are representative of the three ways in which ICA isolated 'KO' in the eight subjects. For each subject the components that contain 'KO' (red), V3 (green) and V5 (blue) are shown superimposed on the individuals' anatomical scans. (A) One of the two subjects in whom 'KO', V3 and V5 were each isolated as separate components. (B) A single subject representative of the five subjects in whom ICA grouped area 'KO' together with V3 in a single component. (C) The subject in whom 'KO' was grouped together with LO. In none of the eight subjects was 'KO' grouped with V5 in the same component.



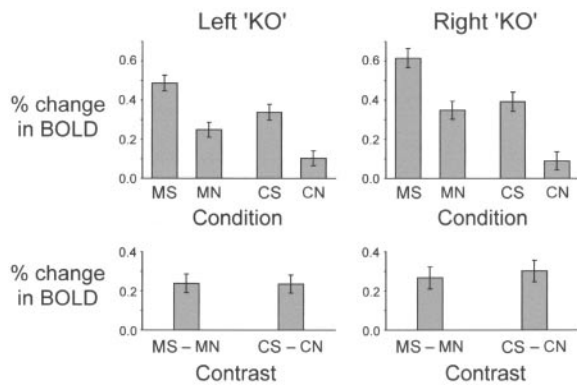


Figure 5. Mean BOLD responses of area KO (left and right) in the four conditions of experiment 1. Bottom row shows shape-specific responses in the context of motion (MS – MN) and of color (CS – CN). BOLD signal is expressed as a percentage of the global mean, with the response to the ‘gray’ baseline conditions subtracted.

with other ones, depending upon its ATC relative to that of other cortical areas. To quantify whether activity in V3B was more related to cortical form-processing or to motion-processing we took the correlation of the blood oxygen level-dependent (BOLD) time-courses between V3B, V5 and V3, obtained during free viewing conditions.

ICA never isolated area V3B together with the motion-sensitive area V5 in the same IC (Fig. 4II). Instead, in six out of eight subjects, it isolated V3B together with areas that have been previously implicated in form perception: with V3 in five subjects, and with LO in one subject. In two subjects it isolated V3B, V5 and V3 in separate ICs. The coordinates of areas V5, V3 and V3B (from eight subjects) are given in Table 2 and correspond closely to those published in earlier studies for these areas (see Materials and Methods). The comparison of the BOLD signal from the hottest voxel in each of these areas revealed that, across all eight subjects, activity in V3B correlated significantly more with that in V3 than with that in V5 (paired *t*-test, $P < 0.0001$) (Fig. 6). We conclude that ‘KO’ (V3B) belongs to the V3 family of areas and is better referred to as ‘V3B’, consistent with the conclusions of Smith *et al.* (Smith *et al.*, 1998).

Physiological Recordings

The above does not provide any evidence for a human visual area specialized for the processing of kinetic contours and shows that the properties of V3B, at least as judged by the similarity of its response to second-order motion stimuli (Smith *et al.*, 1998) and by an analysis of its ATC relative to other areas, are similar to those of V3. It thus seemed interesting to compare these results with our recordings from cells of the third visual complex (V3 and V3A) in the macaque, with the specific aim of learning whether the orientation-selective cells there respond as well to oriented lines generated from luminance and from kinetic contours. In all, we isolated 100 cells that were histologically verified to be in V3 or V3A; all had receptive fields located within the central 10° of the visual field. Seventy-one were orientation selective, and, of these, 52 were studied in greater detail, the rest being excluded because they could not be maintained long enough to complete all tests. Of the 52, three had complex responses to different oriented bars, and seven responded differently to the kinetic and luminance stimuli. The remaining 42 cells responded in a similar way to both, although some preferred oriented lines derived from one or the other. Figure 7 shows the responses and orientation profiles of a cell that responded more vigorously to kinetic boundaries than

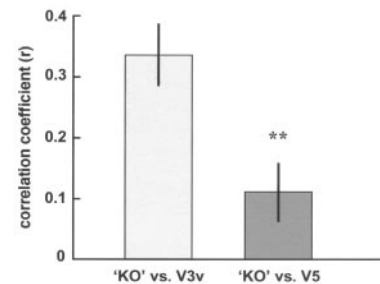


Figure 6. The correlation coefficients of ATCs between areas ‘KO’ and V3 and between ‘KO’ and V5 during free viewing. Lower V3 (V3v) was used in the analysis, as it is spatially further from ‘KO’ than upper V3, and therefore provides a more stringent test. The graph shows the average correlation coefficients r calculated for all pairs of BOLD signal taken from the most significant voxels of areas KO, V5 and V3v within each subject, in the areas identified in all eight subjects. Vertical bars are standard error of the mean (SEM). r of ‘KO’ with V3v ($r = 0.34 \pm 0.05$ SEM) is significantly higher than that of ‘KO’ with V5 ($r = 0.11 \pm 0.05$ SEM) [paired *t*-test, $P < 0.0001$, $n = 28$ (pairs within and across hemispheres)].

luminance ones. Other cells had a preference for luminance boundaries. Figure 8 shows the preferred orientation for each of the 42 cells, with the preferred orientation to a luminance stimulus plotted along the x -axis and the preferred orientation to a kinetic stimulus plotted along the y -axis. The majority of points lie close to the line $x = y$; hence for most cells the preferred orientation is very similar regardless of whether the stimulus is a luminance bar or a kinetic one. Three cells had a bimodal cell response with peaks at 180° intervals and in these the dominant peak for luminance was 180° from the dominant peak for the kinetic contour. The cells’ maximum responses to kinetic and to luminance stimuli are shown in Figure 9; even though the values are more spread on the scatterplot, they are centred along the line $x = y$. When the difference between the luminance and texture responses for each cell is taken, a symmetrical frequency distribution becomes evident (Fig. 9, inset). The frequency distribution is centered near zero, with a slight bias in favor of the luminance stimuli (mean = 15, sample SD = 78). A *t*-test that the mean differs from zero yields a *t*-score of 1.25 ($P = 0.11$, $df = 41$, non-significant). Therefore, even though individual cells may show a strong preference for either luminance or kinetic stimuli, for most cells oriented lines generated from kinetic contours were as effective as those generated from luminance. The same general picture emerges when one looks at the tuning widths (Fig. 10). These are spread out even more on the scatterplot. The differences between the luminance and kinetic contour tuning widths for each cell show a broadly symmetrical frequency distribution (Fig. 10, inset), thus suggesting that most cells have the same tuning widths, whether activated by luminance or kinetic stimuli, even if individual cells sometimes show substantial differences in their tuning widths; the frequency distribution is nevertheless still centered around zero (mean = 0.9429, sample SD = 6.8587). A *t*-test that the mean differs from zero yields a *t*-score of 0.8909 ($P = 0.19$, $df = 41$, non-significant).

We conclude that:

1. For the majority of cells the preferred orientation was very similar whether the stimulus was a luminance bar or a kinetic bar.
2. There was no significant difference in the cell firing rate for luminance and kinetic stimuli when considering the sample as a whole.

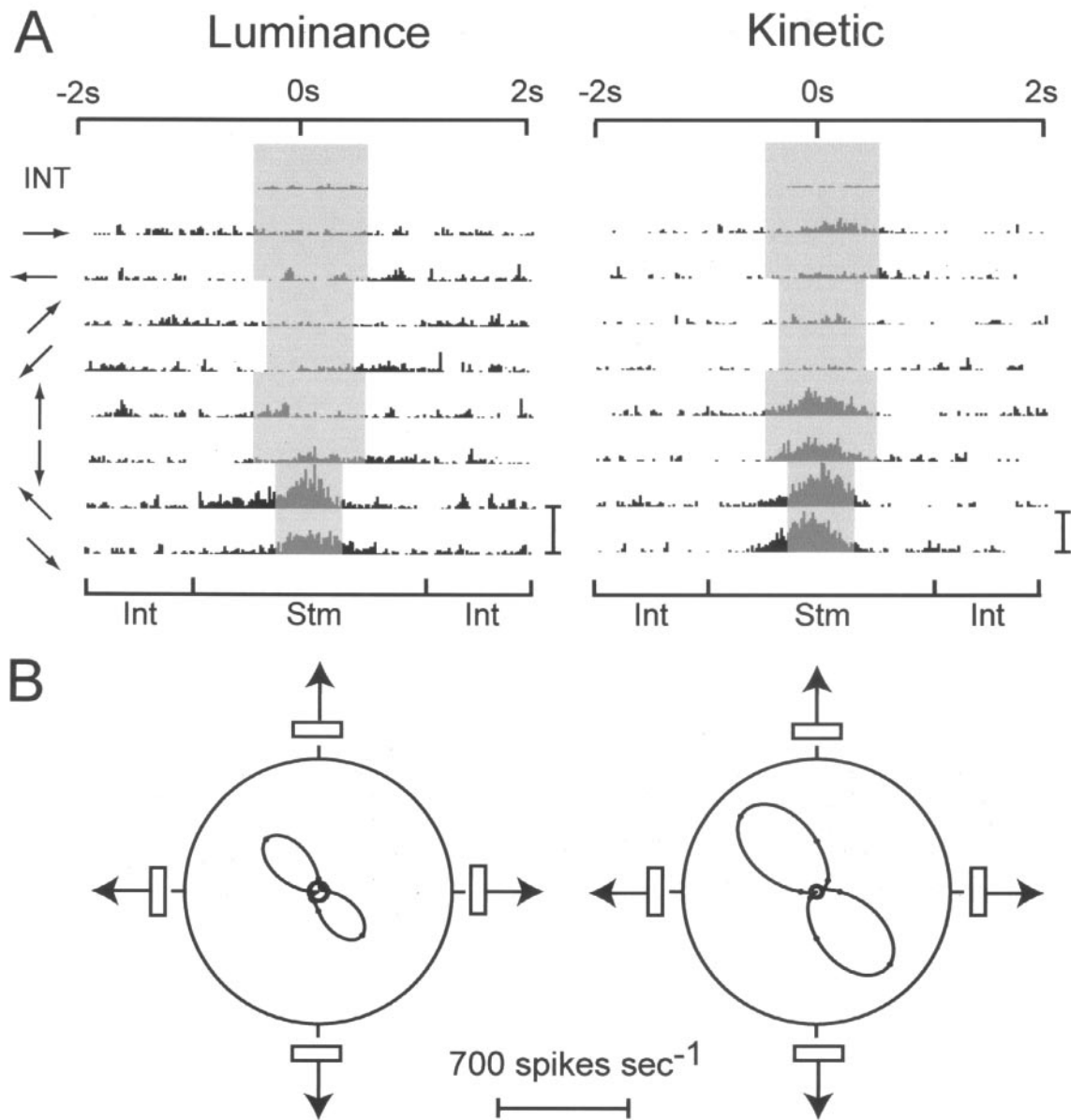


Figure 7. The responses of an orientation-selective cell that favors kinetic contours to motion in different directions of an appropriately oriented bar, defined by luminance (on left) or kinetic contours (on right). In each case, width of stimulus = 0.31° , length = 5.24° , speed = $5.24^\circ/\text{s}$. The responses of the cell are shown in the top two panels (A). Gray areas in each row represent 'response windows', over which the mean firing rate is measured. Top rows show the averaged histograms for 33 interstimulus intervals (INT); the gray response window here is the whole duration of this interval (1s). Each of the other rows shows the mean response to four oriented bars, moving in the direction indicated by the arrow on the left. The gray response window in this case is the period during which the stimulus was in the cell's receptive field. Beneath the histograms, a bar indicates the stimulus interval (Stm), flanked by two interstimulus intervals (Int). Bin width for histograms = 40ms. Scale bars to the right of the histograms represent 1000 spikes/s. The directional profiles of the cell for luminance contours (on left) and kinetic contours (on right) are indicated in the lower two polar plots (B). Solid line shows best spline fit of the data points. Three concentric circles at the centre of each polar plot indicate the background firing rate (from the INT row above), and 1 standard error above and below this firing rate.

- There was no significant difference in the tuning width for luminance and kinetic stimuli when considering the sample as a whole.

Long Penetrations through the Third Visual Complex

Since we were principally interested in the characteristics of the orientation-selective cells within the V3 complex, we did not study in detail the possibility that cells preferring oriented lines generated from luminance or from kinetic boundaries may be grouped together within the cortex. That this may be so is, however, suggested by long oblique penetrations such as the

one illustrated in Figure 11. Of the 20 cells in this penetration (separated from each other by $100\ \mu\text{m}$ on average), six responded better to oriented lines when generated from kinetic contours than when generated from luminance, and three (cells 9, 10, 15) were unselective in that they did not specifically respond to oriented lines. The six that preferred kinetic contours showed some tendency to group together. It is thus possible that there is a subgrouping of cells within the V3 complex, which might imply that a specialization for kinetic contours is not between areas but embedded within an area, an interesting possibility for future studies.

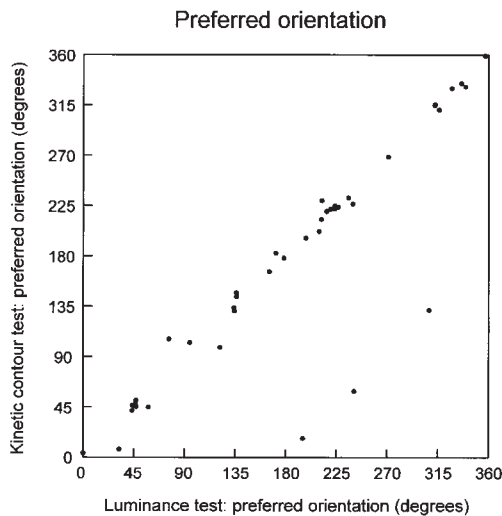


Figure 8. The preferred orientation for each cell, with the preferred orientation to a luminance stimulus plotted along the x-axis and the preferred orientation to a kinetic contour stimulus plotted along the y-axis.

Discussion

The experiments described here revolve around a question of broad interest in studies of the visual brain, namely the extent to which a brain area that is specialized for processing and perceiving a given visual attribute is able to draw on signals from any source to construct that attribute. We have studied this by concentrating on simple two-dimensional shapes and oriented lines that can be generated in a multiplicity of ways – from luminance, from kinetic contours and from equiluminant colors. Any sub-specializations that divide this labor between areas, with some being specialized for encoding lines generated from luminance, others from kinetic contours, and yet others from color or from texture, should have become evident from our studies, since functional imaging studies have demonstrated many such specializations in the past. Yet we found no such specialization or sub-specialization, even though we concentrated on color and motion, the two attributes that would have been the most likely to reveal any sub-specializations. Instead, the area that has been considered by Orban's group to be specialized for the processing of kinetic contours (Orban *et al.*, 1995, Dupont *et al.*, 1997; Van Oostende *et al.*, 1997) turns out in our work to be one that is active when subjects view simple shapes, however derived.

The evidence purporting to show a specialization of area 'KO' for kinetic contours is not compelling. The kinetic stimuli reported to activate 'KO' selectively also activated other areas, notably V5 and V3A (Van Oostende *et al.*, 1997). Our data do not show that 'KO' is specific to the presence of kinetic contours, since it gave equal responses to contours from motion and contours from colour (Fig. 5). The data of Van Oostende *et al.* do not appear to provide evidence of such specificity either, in spite of these authors' conclusions (Van Oostende *et al.*, 1997). According to their Figure 4, 'KO' shows a BOLD response to kinetic contours of 1.89%, compared with 1.03% for their preferred kinetic control stimulus (transparent motion without borders). The contour-specific response for kinetic stimuli was therefore 0.86%. The response to static, luminance contours was 1.03%, compared with 0% for their static control stimulus (0% since the other responses are expressed with respect to the response to the static control). The contour-specific response

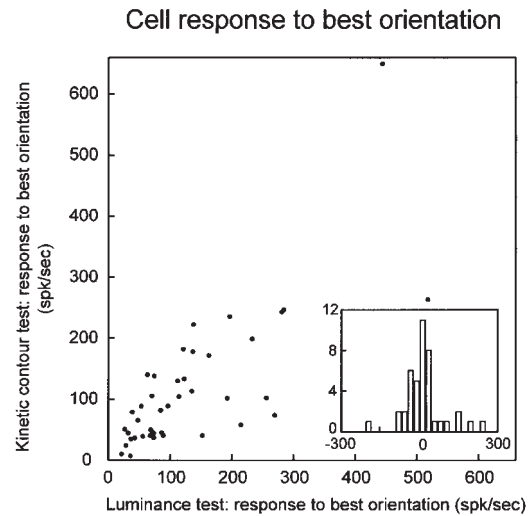


Figure 9. Maximum cell responses for kinetic and luminance contours. The inset graph shows the frequency distribution of the difference between luminance and kinetic responses. In this inset graph, the x-axis shows the difference in response between luminance and kinetic contours (in spikes/s), and the y-axis shows frequency.

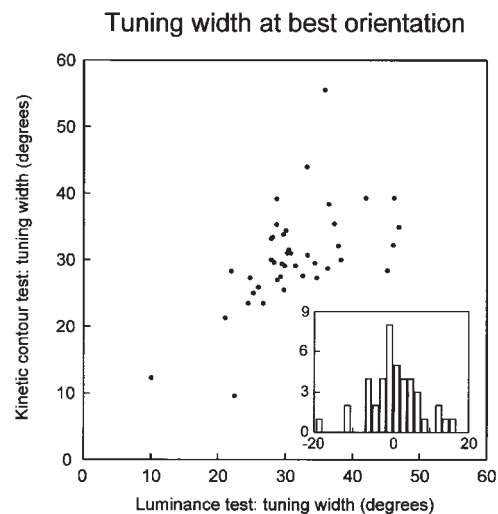


Figure 10. Tuning width of cells at the preferred orientation. The inset graph shows the frequency distribution of the difference between luminance and kinetic contour tuning. In this inset graph, the x-axis shows the difference in tuning between luminance and kinetic contours (in degrees), and the y-axis shows frequency.

for luminance stimuli was therefore 1.03%, i.e. slightly larger than that observed in the kinetic context. Their evidence, thus analyzed, is therefore entirely consistent with ours in showing that V3B (their 'KO') does not give a specific response to kinetic contours. Indeed, together with our data, it shows that V3B responds equally well to isoluminant color contours, luminance contours and kinetic contours.

On the other hand, our ICA analysis shows that the ATC of 'KO' correlates better with that of V3 than that of V5 in free viewing conditions, and, as implied by Smith *et al.* in their use of the term 'V3B' (Smith *et al.*, 1998), it may be better considered to belong to the V3 family of areas. We shall therefore use the term 'V3B' to denote an area in the lateral occipital cortex, located posterior to V5 and in close proximity to the V3 com-

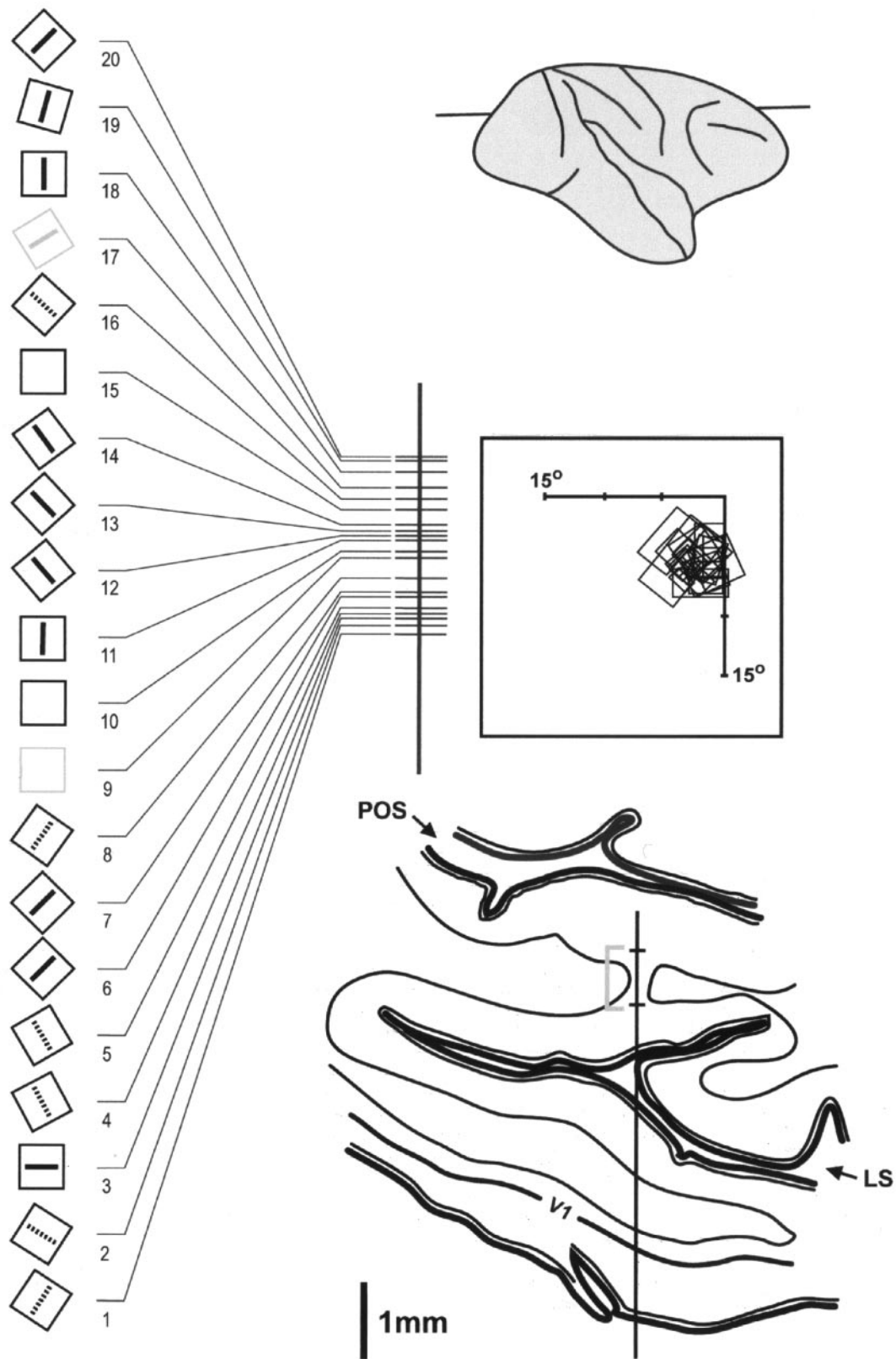


Figure 11. Reconstruction of a long penetration through the annectant gyrus of the lunate sulcus, which houses V3A, shown on a drawing of a horizontal section taken through the posterior part of the brain at the level indicated above. The receptive fields of the 20 cells recorded from were located within the contralateral inferior quadrant, abutting the vertical meridian (centre right of figure). The penetration is reconstructed in detail on the left, showing the receptive fields and the preferences of the cells. Black bars = cells that preferred lines generated from luminance; gray bars = equal response to the two types of stimulus; dashed bars = better response to lines generated from kinetic contours; empty receptive fields signify that the cell was unselective for orientation, but responded better to luminance (cells 10 and 15) or to kinetic contours (cell 9). Average distance between cells was 100 μm . LS, lunate sulcus; POS, parieto-occipital sulcus; V1, primary visual cortex.

plex, whose function cannot be specified at present, but which is closely involved in the processing and extraction of form, however derived, although it may have other functions as well (Poggio *et al.*, 1988; Galletti and Bataglini, 1989; Galletti *et al.*, 1990; Nakamura and Colby, 2000; Adams and Zeki, 2001; Backus *et al.*, 2001). 'Kinetic occipital' does not reflect the function of V3B, and also suggests, erroneously, that there is a cortical specialization for the processing of kinetic contours. Smith *et al.* were probably right in saying that it is 'unsafe to name areas based on assumed functions' (Smith *et al.*, 1998).

Attempts have been made recently to equate human 'KO' with the dorsal part only of area V4 (V4d) in the macaque monkey. Tootell and Hadjikhani used the same stimuli as those of the Orban group to activate the visual brain and concluded that the human V4d 'topologue' 'did respond selectively to kinetic motion boundaries' (Tootell and Hadjikhani, 2001). They were led to this conclusion by comparing the activity produced by kinetic contours with that produced by translational motion. However, they too did not undertake the more critical comparison, of the brain activity produced when subjects view shapes produced from kinetic boundaries and from other attributes, such as color, for example. Their claim of a selectivity for kinetic motion boundaries is therefore also questionable, and is contradicted by our results.

The supposition that 'V4d' alone is the homolog of 'KO' implies that the latter registers activity in lower visual field alone, since V4d represents lower visual fields only. But, the retinotopic studies of Press *et al.* (Press *et al.*, 2001) have shown that both quadrants of the contralateral hemifield are mapped in V3B ('KO') and the same conclusion can be drawn by examining Figure 4 in the work of Smith *et al.* (1998), although the latter authors suppose that lower fields alone are mapped in V3B. The rationale for equating KO with V4d also rests on the unproven supposition that there are areas in the visual brain, such as 'VP' (Burkhalter and Van Essen, 1986) and 'V4v' (Serenio *et al.*, 1995; Hadjikhani *et al.*, 1998) that represent one quadrant of the visual field alone. More recent evidence has, however, called into serious doubt the existence of such areas. The recent detailed retinotopic studies of Wade *et al.*, for example, found no evidence for area 'V4v' but only for an area V4 which abuts area V3 and in which both quadrants are mapped (Wade *et al.*, 2002). 'VP' has also been shown not to exist as a separate area (Rosa *et al.*, 2000; Lyon and Kaas, 2001, 2002); it is instead the upper visual field representation of V3, as originally suggested (Cragg, 1969; Zeki, 1969). Tootell and Hadjikhani have been reassured by the precedent of areas such as 'VP' and 'V4v' into equating 'KO' with V4d alone (Tootell and Hadjikhani, 2001). But given the compelling evidence that areas representing one quadrant of the visual field alone do not exist, areas such as 'VP' and 'V4v' can no longer act as a precedent for other 'improbable' areas and homologies (Zeki, 2003).

That V3B is somewhat more active when simple shapes are generated from luminance or from equiluminant colors than when generated from kinetic contours finds an interesting reflection in the properties of the orientation-selective cells in the V3 complex of the macaque, most of which respond better to the preferred oriented lines when generated from luminance than from kinetic contours. This is also true of other studies (Albright, 1992; Geesaman and Andersen, 1996; Marcar *et al.*, 2000). These have shown that even when a cell maintains its specificity to a stimulus when generated in different ways, the better response is usually to the stimulus generated from luminance differences.

It is interesting to note here a further parallel, that the kinetic

contours in the imaging study of Van Oostende *et al.* (Van Oostende *et al.*, 1997), which used oriented bars, and in ours, which used simple shapes generated from kinetic contours, did not result in any discernible activity within V1 and V2. This very likely reflects the paucity of cells in both areas that respond well to stimuli generated from kinetic contours. They are reported to be rare in V1 and no more than 10% in V2 (Leventhal *et al.*, 1998; Marcar *et al.*, 2000). On the other hand, the majority of orientation-selective cells that we have recorded from in the V3 complex responded to oriented stimuli, however generated. This would suggest that the V3 complex is more heavily involved in the processing of dynamic forms, as suggested from previous evidence (Zeki, 1993).

What is not clear from this, and previous, studies is whether V3B has any homolog in the monkey brain. It would not be surprising if it does not, given the hugely expanded occipital lobe of the human brain. But a possible homolog cannot be ruled out. Some have supposed that the area known as V3A in the human should be subdivided (Press *et al.*, 2001). One of the stranger aspects of this area as originally defined (Van Essen and Zeki, 1978) is the presence of a double representation of central vision, one in the lunate sulcus and the other in the parieto-occipital sulcus. It is possible that each central representation belongs to a separate area, and that part of V3A may have to be fractioned off into a separate area, which may well constitute the monkey homolog of V3B. These are interesting questions to address in the future.

Conclusion

The imaging evidence reported here and by others is no doubt a reflection of the basic physiology of the cerebral cortex, which shows that cells which are selectively responsive to a given feature will respond to that feature no matter how it is derived. This is true of the orientation-selective cells of area V1, for example, which are capable of responding to the same specific orientation whether generated from luminance differences or equiluminant colors, just as the directionally selective cells of V5 are capable of responding to motion in the appropriate direction even when the moving stimulus is made of a color that is equiluminant with the background against which it moves (Saito *et al.*, 1989; ffytche *et al.*, 1995). This general cue-invariance seems to be sufficiently well established in different visual areas – in V1 (Gouras and Kruger, 1979); in V5 (Albright, 1992); in V5A (Geesaman and Andersen, 1996); in the object-selective lateral occipital complex (LOC) (Grill-Spector *et al.*, 1998) and in inferior temporal sulcus (Sary *et al.*, 1993) – for us to accept it as a general strategy used by the cortex. It seems that, given the option of constructing the visual world through the use of a complex strategy or a simple and economical one, the brain has opted for the latter. Rather than assign several areas to signal in several different ways the same attribute when derived from different sources, it has endowed cells within specialized visual areas with the potential of being able to respond to their preferred stimuli in the same specific way, no matter how the stimuli are derived.

Notes

We thank John Romaya for the computer programmes, and Lindsay Wood and Martin Cook for help in preparing the manuscript. The work of this laboratory is supported by the Wellcome Trust, London, UK. Address correspondence to S. Zeki, Wellcome Department of Imaging Neuroscience, University College London, London WC1E 6BT, UK. Email: zeki.pa@ucl.ac.uk.

References

- Adams DL, Zeki S (2001) Functional organization of macaque V3 for stereoscopic depth. *J Neurophysiol* 86:2195–2203.
- Albright TD (1992) Form-cue invariant motion processing in primate visual cortex. *Science* 255:1141–1143.
- Amari S (1998) Natural gradient works efficiently in learning. *Neural Comput* 10:251–276.
- Backus BT, Fleet DJ, Parker AJ, Heeger DJ (2001) Human cortical activity correlates with stereoscopic depth perception. *J Neurophysiol* 86:2054–2068.
- Bartels A and Zeki (2000) The architecture of the colour centre in the human visual brain: new results and a review. *Eur J Neurosci* 12:172–193.
- Bartels A, Zeki S (2001) The chronoarchitecture of the human brain: the dissection of the human brain into functional subdivisions by ICA analysis of fMRI data collected during free viewing of a movie. *Soc Neurosci Abstr* 620.15
- Bartels A, Zeki S (2003) The chronoarchitecture of the human brain. In preparation.
- Bell AJ, Sejnowski TJ (1995) An information maximization approach to blind separation and blind deconvolution. *Neural Comput* 7:1129–1159.
- Burkhalter A, Van Essen DC (1986) Processing of color, form and disparity information in visual areas VP and V2 of ventral extrastriate cortex in the macaque monkey. *J Neurosci* 6:2237–351.
- Burkhalter A, Felleman DJ, Newsome WT, Van Essen DC (1986) Anatomical and physiological asymmetries related to visual areas V3 and VP in macaque extrastriate cortex. *Vision Res.* 26:63–80
- Callaway EM (1998) Local circuits in primary visual cortex of the macaque monkey. *Annu Rev Neurosci* 21:47–74.
- Casagrande VA, Kaas JH (1994) The afferent, intrinsic and efferent connections of primary visual cortex in primates. In: *Cerebral cortex* (Peters A, Rockland K eds), Vol. 10, pp. 201–256. New York: Plenum Press.
- CIE (1931) Commission Internationale de l’Eclairage (CIE)/ Proceedings, International Congress on Illumination, Cambridge: Cambridge University Press.
- Cragg BG (1969) The topography of the afferent projections in circumstriate visual cortex studied by the Nauta method. *Vision Res.* 9:733–747
- DeYoe EA, Carman GJ, Bandettini P, Glickman S, Wieser J, Cox R, Miller D, Neitz J (1996) Mapping striate and extrastriate visual areas in human cerebral cortex. *Proc Natl Acad Sci USA* 93:2382–2386.
- Dupont P, de Bruyn B, Vandenberghe R, Rosier A, Michiels J, Marchal G, Mortelmans L, Orban GA (1997) The kinetic occipital region in human visual cortex. *Cereb Cortex* 7:283–292.
- ffytche DH, Skidmore BD, Zeki S (1995) Motion-from-hue activates area V5 of human visual cortex. *Proc R Soc Lond B* 260:353–358.
- Frackowiak RSJ, Zeki S, Poline JB, Friston KJ (1996) A critique of a new analysis proposed for functional neuroimaging. *Eur J Neurosci* 8:2229–2231.
- Friston KJ, Frith CD, Frackowiak RSJ, Turner R (1995) Characterizing dynamic brain responses with fMRI – a multivariate approach. *Neuroimage* 2:166–172.
- Friston KJ, Holmes AP, Worsley KJ (1999) How many subjects constitute a study? *Neuroimage* 10:1–5.
- Galletti C, Battaglini PP (1989) Gaze-dependent visual neurons in area V3A of monkey prestriate cortex. *J Neurosci* 9:1112–1125.
- Galletti C, Battaglini PP, Fattori P (1990) ‘Real-motion’ cells in area V3A of macaque visual cortex. *Exp Brain Res* 82:67–76.
- Geesaman BJ, Andersen RA (1996) The analysis of complex motion patterns by form/cue invariant MSTd neurons. *J Neurosci* 16:4716–4732.
- Gouras P, Kruger J (1979) Responses of cells in foveal striate cortex of the monkey to pure color contrast. *J Neurophysiol* 42:850–860.
- Grill-Spector K, Kushnir T, Edelman S, Itzhak Y, Malach R (1998) Cue-invariant activation in object-related areas of the human occipital lobe. *Neuron* 21:191–202.
- Gulyas B, Heywood CA, Popplewell DA, Roland PE, Cowey A (1994) Visual form discrimination from color or motion cues: functional anatomy by positron emission tomography. *Proc Natl Acad Sci USA* 91:9965–9969.
- Hadjikhani N, Liu AK, Dale A, Cavanagh P, Tootell RBH. (1998) Retinotopy and color sensitivity in human visual cortical area V8. *Nature Neurosci* 1:235–241.
- Josephs O, Turner R, Friston K (1997) Event-related fMRI. *Hum Brain Mapp* 5:243–248.
- Kaiser PK (1991) Flicker as a function of wavelength and heterochromatic flicker photometry. In: *Limits of vision* (Kulikowski JJ, Walsh V, Murray IJ, eds), pp. 171–190. Basingstoke: Macmillan.
- Leventhal AG, Wang Y, Schmolensky MT, Zhou Y (1998) Neural correlates of boundary perception. *Vis Neurosci* 15:1107–1118.
- Lund JS, Yoshioka T, Levitt JB (1994) Substrates for interlaminar connections in area V1 of macaque monkey cerebral cortex. In: *Cerebral cortex* (Peters A, Rockland K, eds), Vol. 10, pp. 37–60. New York: Plenum Press.
- Lyon DC, Kaas JH (2001) Connectional and architectonic evidence for dorsal and ventral V3, and dorsomedial area in marmoset monkeys. *J Neurosci* 21:249–261.
- Lyon DC, Kaas JH (2002) Evidence for a modified V3 with dorsal and ventral halves in macaque monkeys. *Neuron* 33:453–461.
- Makeig S, Jung TP, Bell AJ, Ghahremani D, Sejnowski TJ (1997) Blind separation of auditory event-related brain responses into independent components. *Proc Natl Acad Sci USA* 94:10979–10984.
- Malach R, Reppas JB, Benson RR, Kwong KK, Jiang H, *et al.* (1995) Object-related activity revealed by functional magnetic-resonance-imaging in human occipital cortex. *Proc Natl Acad Sci USA* 92:8135–8139.
- Marcar VL, Raiguel SE, Xiao D, Orban GA (2000) Processing of kinetically defined boundaries in areas V1 and V2 of the macaque monkey. *J Neurophysiol* 84: 2786–2798.
- McKeown MJ, Makeig S, Brown GG, Jung TP, Kindermann SS, *et al.* (1998) Analysis of fMRI data by blind separation into independent spatial components. *Hum. Brain Mapp* 6:160–188.
- Nakamura K, Colby CL (2000) Visual, saccade-related, and cognitive activation of single neurons in monkey extrastriate area V3A. *J Neurophysiol* 84:677–692.
- Okusa T, Kakigi R, Osaka N (2000) Cortical activity related to cue-invariant shape perception in humans. *Neuroscience* 98:615–624.
- Orban GA, Sary G, Vogels R, Orban GA (1993) Cue-invariant shape selectivity of macaque inferior temporal neurons. *Science* 260: 995–997.
- Orban GA, Dupont P, DeBruyn B, Vogels R, Vandenberghe R, Mortelmans L (1995) A motion area in human visual cortex. *Proc Natl Acad Sci USA* 92: 993–997.
- Perry RJ, Zeki S (2000) Integrating motion and colour within the visual brain: an fMRI approach to the binding problem. *Soc Neurosci Abstr* 250.1.
- Poggio GF, Gonzalez F, Krause F. 1988. Stereoscopic mechanisms in monkey visual cortex – binocular correlation and disparity selectivity. *J Neurosci* 8:4531–4550.
- Press WA, Brewer AA, Dougherty RF, Wade AR, Wandell BA (2001) Visual areas and spatial summation in human visual cortex. *Vis Res* 41:1321–1332.
- Roland PE, Gulyas B (1996) Assumptions and validations of statistical tests for functional neuroimaging. *Eur J Neurosci* 8:2232–2235.
- Rosa MG, Pinon MC, Gattass R, Sousa AP (2000) ‘Third tier’ ventral extrastriate cortex in the New World monkey, *Cebus apella*. *Exp Brain Res* 132:287–305.
- Saito H, Tanaka K, Isono H, Yasuda M., Mikami A (1989) Directionally selective response of cells in the middle temporal area (MT) of the macaque monkey to the movement of equiluminous opponent colour stimuli. *Exp Brain Res* 75:1–14.
- Sary G, Vogels R, Orba GA (1993) Cue-invariant shape selectivity of macaque inferior temporal neurons. *Science* 260:995–997.
- Schanze, T (1995) Sinc interpolation of discrete periodic signals. *IEEE Trans. Sig Process.* 43:1502–1503.
- Sereno MI, Dale AM, Reppas JB, Kwong KK, Belliveau JW *et al.* (1995) Borders of multiple visual areas in humans revealed by functional magnetic resonance imaging. *Science* 268:889–893.
- Shipp S, Zeki S (1989) The organization of connections between V5 and V1. *Eur J Neurosci* 1:333–354.
- Shipp S, Watson JDG, Frackowiak RSJ, Zeki S (1995) Retinotopic maps in human prestriate visual cortex: The demarcation of areas V2 and V3. *Neuroimage* 2:125–132.
- Smith AT, Greenlee MW, Singh KD, Kraemer FM, Hennig J (1998) The processing of first- and second-order motion in human visual cortex assessed by functional magnetic resonance imaging (fMRI). *J Neurosci* 18:3816–3830.

- Talairach J, Tournoux P (1988) Co-planar stereotaxic atlas of the human brain. Stuttgart: Thieme-Verlag.
- Tootell RB, Dale AM, Sereno MI, Malach R (1996) New images from human visual cortex. *Trends Neurosci* 19:481-489.
- Tootell RB, Hadjikhani N (2001) Where is 'dorsal V4' in human visual cortex? Retinotopic, topographic and functional evidence. *Cereb Cortex* 11:298-311.
- Tootell RBH, Mendola JD, Hadjikhani NK, Ledden PJ, Liu AK, Reppas JB, Sereno MI, Dale AM (1997) Functional analysis of V3A and related areas in human visual cortex. *J Neurosci* 17:7060-7078.
- Van Essen DC, Zeki SM (1978) The topographic organization of rhesus monkey prestriate cortex. *J Physiol* 277:193-226.
- Van Oostende S, Sunaert S, Van Hecke P, Marchal G, Orban GA (1997) The kinetic occipital (KO) region in man: an fMRI study. *Cereb Cortex* 7:690-701.
- Wade AR, Brewer AA, Rieger JW, Wandell BA (2002). Functional measurements of human ventral occipital cortex: retinotopy and color. *Phil Trans R Soc Lond B* (in press).
- Watson JDG, Myers R, Frackowiak RSJ, Hajnal JV, Woods RP, *et al.* (1993) Area V5 of the human brain: evidence from a combined study using positron emission tomography and magnetic resonance imaging. *Cereb Cortex* 3:79-94.
- Zeki S (1969) Representation of central visual fields in prestriate cortex of monkey. *Brain Res* 14:271-291.
- Zeki S (1978) The third visual complex of rhesus monkey prestriate cortex. *J Physiol* 277:245-272.
- Zeki S (1978) Uniformity and diversity of structure and function in rhesus monkey prestriate cortex. *J Physiol* 277:273-290.
- Zeki S (1991) Parallelism and functional specialization in human visual cortex. *Cold Spring Harb Symp Quant Biol* 55:651-661.
- Zeki S (1993) *A Vision of the Brain*. Oxford: Blackwell.
- Zeki S (2003) Improbable areas in the visual brain. *Trends Neurosci* (in press).
- Zeki S, Shipp S (1988) The functional logic of cortical connections. *Nature* 335:311-317.
- Zeki S, Shipp S (1989) The organization of connections between V4 and V2. *Eur J Neurosci* 1:494-506.
- Zeki S, Watson JDG, Lueck CJ, Friston KJ, Kennard C, Frackowiak RSJ (1991) A direct demonstration of functional specialization in human visual cortex. *J Neurosci* 11:641-449.